Identification of red blood cell membrane defects in a patient with hereditary spherocytosis using next-generation sequencing technology and matrix-assisted laser desorption/ionization time-of-flight mass spectrometry

LEYLA TÜRKER ŞENER[1], MELİH AKTAN[2], GÜRCAN ALBENİZ[3], AZİZ ŞENER[4], DURAN ÜSTEK[5] and IŞIL ALBENİZ[1]

Departments of [1]Biophysics and [2]Hematology, Istanbul Faculty of Medicine, Istanbul University, 34093 Istanbul; [3]Department of General Surgery, Cerrahpaşa Faculty of Medicine, Istanbul University Cerrahpaşa, 34096 Istanbul; [4]Department of General Surgery, Kanuni Sultan Suleyman Training and Research Hospital, 34303 Istanbul; [5]Department of Medical Genetics and REMER, Medipol University, 34810 Istanbul, Turkey

Received June 22, 2018; Accepted February 13, 2019

DOI: 10.3892/mmr.2019.10036

Abstract. Hereditary spherocytosis (HS) is characterized by the morphological transformation of erythrocytes into a spherical shape due to a hereditary defect in cell membrane proteins (ghosts) associated with disruption of erythrocyte skeletal structures. Contrary to the literature, pores were detected in the erythrocytes of a patient with HS. The aim of the present study was to determine the affected proteins and genes that were responsible for the pores. Ghost isolation was performed to determine the proteins responsible for the pores observed on the erythrocytes of the patient. Erythrocyte membrane proteins were visualized using SDS-PAGE. Exome and matrix-assisted laser desorption/ionization time-of-flight mass spectrometry (MALDI TOF MS) analyses were used to identify the genes and proteins responsible for the observed defect. Quantitative protein assessments were performed using MALDI TOF MS. A difference was detected in the components of the erythrocyte membrane proteins. Band 3 and protein 4.2, which serve a particular role in membrane structure, decreased 4.573 and 4.106 fold, respectively. Through proteomic analyses, a non-synonymous exonic mutation region was identified in the Golgi membrane protein 1 (GOLM1) gene (Chr9 rs142242230). Sorting Intolerant From Tolerant and Polymorphism Phenotyping Scores, Likelihood Ratio Tests and MutationTaster revealed that the mutation was deleterious. The pores observed in the morphology of the erythrocytes may have developed due to the decrease in these proteins, which reside in the erythrocyte membrane structure. Furthermore, genetic profiling of the patient with HS and her family was conducted in the present study. Next-generation sequencing was used, and the genetic source of HS was identified as a GOLM1 gene mutation. The assessment of specific molecular defects is often not performed as the majority of mutations are unique to a family. However, molecular analyses should be performed in severe cases where prenatal diagnosis is required, or for unique HS phenotypes to aid scientific investigation.

Correspondence to: Professor Işil Albeniz, Department of Biophysics, Istanbul Faculty of Medicine, Istanbul University, Millet Street, 34093 Istanbul, Turkey
E-mail: ialbeniz@istanbul.edu.tr

Key words: hereditary spherocytosis, matrix-assisted laser desorption/ionization time-of-flight mass spectrometry, next-generation sequencing, exome capture, scanning electron microscopy

Introduction

Hereditary spherocytosis (HS) is an inherited hemolytic anemia that emerges as a result of a defect in erythrocyte membrane proteins, and is characterized by spherocytes in the peripheral blood (1). Clinically, HS is characterized by anemia, jaundice and splenomegaly to various degrees. Common complications are cholelithiasis, hemolytic episodes and aplastic crisis (2). HS has been documented across all races and ethnic groups. The prevalence is 1:5,000 in Northern European countries (3). Autosomal dominant inheritance is observed in 80% of patients and autosomal recessive in the remainder. Homozygote dominant HS is nearly lethal. *De novo* mutations of erythrocyte membrane protein genes (ankyrin, β-spectrin or band 3 genes) are prevalent in HS (4). Autosomal recessive inheritance is associated with mutations of the α-spectrin or protein 4.2 genes (4-6).

Erythrocyte membrane proteins are divided into two groups: Peripheral proteins and integral (transmembrane) proteins. Spectrin accounts for 50% of the peripheral proteins. Spectrin tetramers anchor to protein 4.1 and actin via their tails, and combine with band 3, which moves to the outer surface of the lipid layer by anchoring to Ankyrin (4). In addition, band 3 regulates water and anion transport in the cell

membrane (5,6). Normal qualitative and quantitative levels of erythrocyte membrane proteins are important for membrane stabilization through their connections to the lipid layer (7,8). Quantitative and qualitative deficits lead to lipid loss from the erythrocyte surface and to decreases in erythrocyte surface volume ratio, normal shape, heat and mechanical stability. The osmotic fragility of the erythrocytes is also negatively affected, resulting in a shortened life span and hemolytic anemia (9).

Decreased levels of membrane proteins, which are not identifiable with electrophoretic analyses, cause abnormal cell morphology, osmotic fragility and other erythrocyte defects (8). Quantitative protein assessments have been performed using matrix-assisted laser desorption/ionization-time of flight mass spectrometry (MALDI TOF MS) to identify the membrane protein defects. MALDI is one of the primary sensitive ionizer methods used as an ion source in mass spectrometry, and biomolecules, including proteins, are easily be ionized (10).

Next-generation DNA sequencing (NGS) technology facilitates access to substantial and unique information about genetic/epigenetic regulatory networks, chromatin structure, nuclear organization and genome variations, none of which are provided by other experimental methods. Ultra-speed sequencing is achievable through genome transcription and DNA-protein interactions analyses with highly accurate results (11).

The present study aimed to analyze the genetic profile of a patient, a 35 year old woman who had undergone laparoscopic splenectomy due to severe HS, and her family members. In order to identify the genetic basis for erythrocyte membrane protein deficits, MALDI TOF MS and NGS methods were used to understand the pathophysiological mechanism in HS.

Materials and methods

Ethics and subject information. The Ethics Committee of the Istanbul Faculty of Medicine, Istanbul University (Istanbul, Turkey) approved the study, and written informed consent was obtained from all subjects prior to sample collection. The laboratory characteristics of the patient with hereditary spherocytosis (E.U) were analyzed via a blood test performed prior to splenectomy (Table I). The osmotic fragility test is common in hematology, and is often performed to aid with diagnosis of diseases associated with RBC membrane abnormalities. The osmotic fragility test is used to measure the level of hemolysis in a collected sample of a patient's blood which is compared to a control sample. For an osmotic fragility test, blood sample was usually collected from the right arm from patients. Red blood cells were lysed in a 0.9% NaCI salt solution. Providing the patient's red blood cells are more fragile than normal, a positive result is obtained (12).

The HS patient featured in the present study is a 35 year old woman diagnosed a with deep vein thrombosis and cardiac problem. The healthy control group was composed of 3 female subjects (34, 35 and 63 years old) and 3 male subjects (28, 34 and 58 years old). DNA samples were also collected from the mother (64 years old), father (66 years old) and son (12 years old) of the patient. Samples were collected in January 2015 to April 2015.

All clinical investigations were conducted in accordance with the principles of the Declaration of Helsinki. The parents gave informed consent for publication of this study. The study was approved by the research fund of Istanbul University (project no. 35214; date, 2015).

Preparation of red blood cell ghost. Red blood cell (RBC) membrane ghosts were prepared in accordance with the methods of Dodge *et al* (13). Erythrocytes were isolated by centrifugation for 20 min at 314 x g at room temperature. The packed cells were lysed in of cold 5 mM sodium phosphate. RBC preparations were washed three times in 5 mM sodium phosphate, and centrifuged at 20,070 x g at 4˚C (Heraeus Megafuge 1.0R; Heraeus Deutschland GmbH & Co., Hanau, Germany). The cells were hypotonically lysed and washed free of hemoglobin, with the resulting membrane ghosts consisting solely of the lipid bilayer and associated proteins.

SDS-PAGE of RBC membrane. Erythrocyte ghosts were separated by SDS-PAGE (14). The stacking gel was prepared at room temperature using 4% acrylamide (Sigma-Aldrich; Merck KGaA, Darmstadt, Germany) Tris-HCl (0.5 M pH 6.8; Sigma-Aldrich), containing 0.4% SDS, and the separating gel was prepared at room temperature using 10% acrylamide Tris-HCl buffer (1.5 M, pH 8.8), containing 0.4% SDS (Sigma-Aldrich). After spectrophotometric measurements were obtained, each sample (20 μg) was mixed with the sample buffer to a final concentration of 0.06 M Tris-HCl pH 6.8, 2% SDS, 5% β-mercaptoethanol, 10% glycerol and 0.025% bromophenol blue. Following electrophoresis, the gels were fixed for 1 h in a solution of 40% (v/v) aqueous ethanol (99.8%; Sigma-Aldrich) and 10% (v/v) acetic acid (Merck KGaA) at room temperature. The gels were then washed for 30 min in fresh fixing solution and incubated with Coomassie Blue R-250 0.2% diluted in fixative solution for 2 h at room temperature (Thermo Fisher Scientific, Inc., Waltham, MA, USA). The gels were destained using fixative solution for 2 h, followed by incubation in water at room temperature until complete destaining.

May-Grünwald giemsa staining. A drop of anticoagulated blood was dripped on the far end of a microscope slide. A second slide was dragged forward with a quick, smooth movement to produce a 2-3 cm smear. Staining was performed when the preparations were dry.

The microscope slide was covered with May-Grünwald stain for 3 min at room temperature. The slide was held from one end, and the residual stain drained and removed with distilled water. The slide was placed horizontally and covered with distilled water. Giemsa stain was dripped on the distilled water (2-3 drops) and allowed to stand for 8 min, following which the residual stain was drained and washed with tap water. The preparation was analyzed under a light microscope when the slide was dry (15).

Scanning electron microscopy (SEM). Blood samples were centrifuged at 706 xg (rotor diameter, 16 cm) 5 min at room temperature. Erythrocyte samples for the scanning electron microscopy were fixed for 24 h in 2.5% glutaraldehyde in 0.1 M phosphate buffer at pH 7.4 at room temperature. The samples were dehydrated via a gradual increase in concentrations of ethanol and amile acetate; they were then dried at critical-point in a Balzers

Table I. Blood test results of the patient with hereditary spherocytosis.

Parameter	Patient results
Hemoglobin, g/dl	6.8
Hematocrit, %	18
Bilirubin, mg/dl	3.61
Lactate dehydrogenase, U/l	323
Leukocyte, mm^3	2,300
Platelets, mm^3	194,000

Osmotic fragility increase.

critical point drier using liquid CO_2. The cells were settled on coverslips (Assistent; Glaswarenfabrik Karl Hecht Kg, Sondheim, Germany) using a Shandon Cytospin 2 (200 x g 5 min at room temperature; Dako; Agilent Technologies, Inc., Santa Clara, CA, USA), followed by dehydration using increasing concentrations of ethanol. Finally, the samples were sputter coated with 3 nm of gold using the BAL-TEC MED 020 (Leica Microsystems GmbH, Wetzlar, Germany) coating system and analyzed with a FEI Quanta 450 FEG-EDS (FEI; Thermo Fisher Scientific, Inc.) scanning transmission electron microscope.

Proteome analysis of erythrocyte membrane. Ghost materials from the patient and healthy subjects were frozen with liquid nitrogen and pulverized with a bead beater (Mixer Mill MM301; Retsch GmbH, Haan, Germany). A volume of 500 μl of UPX™ universal protein extraction buffer (Expedeon, Heidelberg, Germany) with 5 μl protease inhibitor cocktail (Sigma-Aldrich; Merck KGaA) was added to samples and boiled at 100˚C for 5 min, and subsequently centrifuged at 15.366 x g for 15 min to remove the debris. The supernatant was transferred to a clean tube and protein concentration was measured with a NanoDrop™ spectrophotometer (ND-1000; NanoDrop Technologies; Thermo Fisher Scientific, Inc., Wilmington, DE, USA) at 280 nm. Tryptic peptides were generated in accordance with the filter-aided sample preparation protocol (16). Peptides were eluted from the spin column, the concentration was measured with a NanoDrop™ spectrometer, adjusted to a concentration of 100 ng/μl, and 50 fmol internal standards (MassPREP Enolase Digestion Standard; Waters Corporation, Milford, MA, USA).

Liquid chromatography-mass spectrometry (LC-MS/MS) analysis and database search. LC-MS/MS analysis and protein identifications were performed according to a previously published protocol (17). In brief, 500 ng of tryptic peptides in 5 μl for each experimental condition were analyzed using the LC-MS/MS system (nanoACQUITY ultra pressure liquid chromatography, SYNAPT high definition mass spectrometer, NanoLockSpray mass ionization source; Waters Corporation). Columns were equilibrated with 97% mobile phase A (0.1% formic acid in LC-MS grade water; Sigma-Aldrich; Merck KGaA) and the column temperature was set to 45˚C. The peptides were separated from the trap column (Symmetry C18 5 μm, 180 μm i.d. x 20 mm; Waters Corporation) by gradient elution into an analytical column (BEH C18, 1.7 μm, 75 μm i.d. x 250 mm; Waters Corporation) at a 300 nl/min flow rate, with a linear gradient from 5-40% mobile phase B (0.1 formic acid in hypergrade acetonitrile; Sigma-Aldrich; Merck KGaA) over 90 min.

Data independent acquisition was performed by operating the instrument at positive ion V mode, applying the MS and MS/MS functions over 1.5 sec intervals with 6 V low energy and 15-40 V high energy collision. Glu-fibrinopeptide (internal mass calibrant) was infused every 45 sec at 300 nl/min flow rate. Values of mass charge ratio (m/z)>50-1,600 were recorded. Tandem mass data extraction, charge state deconvolution and deisotoping were conducted using ProteinLynx Global Server v2.5 (Waters Corporation), and searched with the Identity^E High Definition Proteomics System (Waters Corporation), using a fragment ion mass tolerance of 0.025 Da and a parent ion tolerance of 0.0100 Da against the reviewed human protein database from Uniprot (18). The amino acid sequence of the internal standard (yeast enolase; Uniprot accession no. P00924) was included in the FASTA file of the database. The Apex 3D data preparation parameters were set to 0.2 min chromatographic peak width, 10.000 MS TOF resolution, 150 counts for low energy threshold, 50 counts for elevated energy threshold, and 1,200 counts for the intensity threshold. The databank search query was set to a minimum 3 fragment ion matches per peptide, minimum 7 fragment ion matches per protein, minimum 1 peptide matches per protein and 1 missed cleavage. Carbamidomethyl-cysteine fixed modification and Acetyl N-TERM, deamidation of asparagine and glutamine, and oxidation of methionine variable modifications were set. Quantification of the protein expression changes were performed with Progenesis LC-MS software V4.0 (Nonlinear Dynamics; Waters Corporation). Normalization across the sample set was based on the total ion signal. Protein quantitation was only performed with non-conflicting peptide features.

Exome capture/massively parallel sequencing. DNA was extracted from 1 ml venous blood (MagNA Pure Compact Nucleic Acid Isolation kit; Roche Applied Science, Penzberg, Germany). DNA Purity and integrity were checked using a spectrophotometer (ND-1000, NanoDrop™) and 1% agarose gel electrophoresis, respectively (19). The quantity of genomic DNA was measured using a sensitive fluorescence-based kit (Qubit RNA BR assay kit, Invitrogen; Thermo Fisher Scientific, Inc) and an integrated instrument (Qubit 2.0 Fluorometer; Invitrogen; Thermo Fisher Scientific, Inc). Genomic DNA (1,500 ng) was fragmented with an ultrasonicator (S220; Covaris, Inc., Woburn, MA, USA) following the manufacturer's instructions for a target peak of 400 bp. Libraries were prepared using TruSeq DNA Sample Preparation Kit-Set A (Illumina, Inc., San Diego, CA, USA). Following three subsequent steps (end repair, A-tailing and adaptor ligation), DNA fragments (~400-550 bp) were separated with the E-Gel SizeSelect 2% Agarose system (Invitrogen; Thermo Fisher Scientific, Inc), purified using MinElute Gel Extraction kit (Qiagen, Inc., Valencia, CA, USA), and amplified by polymerase chain reaction (PCR), according to the sample preparation guide. Exonic regions were isolated using TruSeq Exome Enrichment kit in accordance with manufacturer's guidelines (Illumina, Inc.). This process includes two hybridization steps using capture target oligos and streptavidin beads to enrich exonic regions,

and wash steps to eliminate non-specific binding from the beads. Cluster generation from a DNA template was performed with an automated system (cBot; Illumina, Inc.) using TruSeq PE Cluster kit V3 (Illumina, Inc.). Sequencing (multiplexed paired-end) was performed with HiSeq 2000 (Illumina, Inc.) using TruSeq SBS kit v3 (200 cycles) (Illumina, Inc.). Illumina Real-Time Analysis software (version 1.13) with standard parameters was used for real-time image analysis and base calling (Illumina, Inc.). At the end of all procedures, 104-bp-long paired-end reads were obtained.

Exome sequencing analysis pipeline. Raw sequencing data were aligned to the human genome hg19 reference using Burrows-Wheeler Aligner (20) with standard parameters in paired-end mode. SAMtools (21) was used to remove the PCR duplicates. BEDtools (22) was used to calculate the coverage of targeted exome regions. A total of 82% of targeted regions were covered at least nine times, and the average sequencing depth of the regions was 24-fold. These values are the mean of all samples. Genome Analysis Toolkit v1.6 (GATK) was used for local realignment around indels (23). Indel Realigner was used, and single nucleotide polymorphisms and small indels were called using a GATK Unified Genotyper (24). ANNOVAR (25) was used for functional annotation of variants including gene/exonic region, segmental duplications, sorting intolerant from tolerant (SIFT), MutationTaster and Polymorphism Phenotyping (PolyPhen) scores (26).

Statistical analysis. All experiments were conducted at least in triplicate. Statistical analysis was performed and data are presented as the mean ± standard deviation. For comparisons of two normally distributed groups, a Student's t-test was used. $P<0.05$ was considered to indicate a statistically significant difference. All statistical analyses were performed using SPSS (version 21; IBM Corp., Armonk, NY, USA).

Results

Clinical profile of the patient. Splenectomy and cholecystectomy were performed when the patient had been diagnosed with HS. The results of blood tests performed post-splenectomy were as follows: Hemoglobin (Hb), 9.2 g/dl; hemotocrit (Hct), 27%; leucocyte, 8,500/mm^3; platelets, 1,300,000/mm^3. Hemoglobin A_2 was determined as 3.7% using an LH 780 Hematology analyzer (Beckman Coulter, Inc., Brea, CA, USA).

May-Grünwald Giemsa staining and SEM images of the RBCs of the patient. The arrows in Fig. 1A indicate the localization of the pores assumed in the patient's RBCs following May-Grünwald Giemsa staining. As presented in Fig. 1B May-Grünwald staining indicated the localization of healthy RBCs following Giemsa staining. There was no porous structure in healthy RBCs. These morphological abnormalities were subsequently confirmed using SEM. The presence of these pores in the membrane is inconsistent with the literature (Fig. 2). SDS-PAGE analysis of the erythrocyte membrane proteins was performed to identify the responsible genes and proteins for these defects.

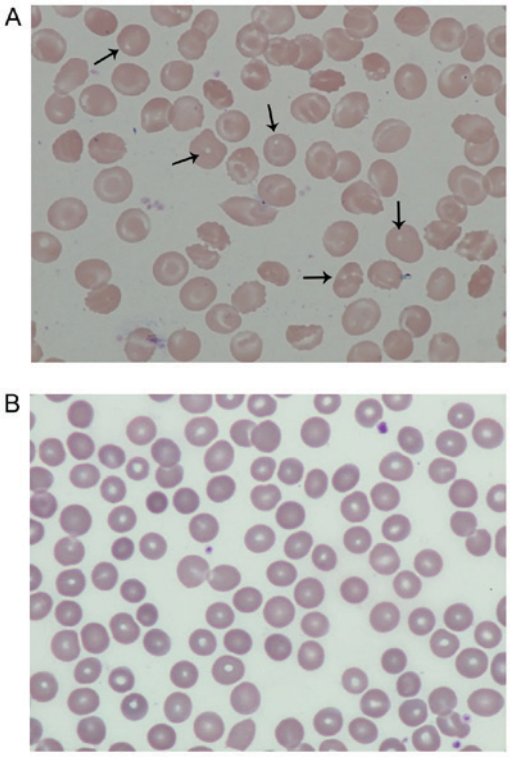

Figure 1. Smear preparation with May-Grünwald staining. (A) Patient with hereditary spherocytosis. The smear preparation was obtained when the anticoagulated blood sample had been drawn. The arrows indicate the localization of pores. (B) Healthy erythrocyte membrane proteins of the control group. Magnification, x10,000.

SDS-PAGE and proteome analyses of erythrocyte membrane proteins. Blood samples were collected from the patient who was admitted to the Hematology Clinic at Istanbul Medical Faculty (Istanbul, Turkey) and diagnosed as having congenital hemolytic anemia. Erythrocyte membrane protein (ghost) isolation was performed from the patient's blood sample from the healthy control group. Erythrocyte membrane proteins were subsequently screened using polyacrylamide SDS-PAGE electrophoresis (Fig. 3). Abnormal morphology of the RBCs may have affected the results of the SDS-PAGE gel, and therefore direct comparisons of the healthy group and the HS patient are not possible. Quantitative protein assessments were conducted using MALDI TOF MS to accurately determine the membrane protein deficits.

The results of the MALDI TOF MS analysis revealed the majority of the bands, particularly spectrin and ankyrin, had a reduction in the amount of membrane proteins compared with the controls. Band 3, which has a notable role in membrane structure, decreased 4.573-fold, and protein 4.2 decreased 4.106-fold compared with healthy controls. Quantitative protein amounts (ng) with MALDI TOF MS are shown in Table II.

Confirmation of the decrease in the amount of erythrocyte proteins verified in the SDS-PAGE analysis, is presented in Figs. 4 and 5.

To further characterize the RBC proteome of the patient, blood samples from the patient and family (Fig. 6) were collected and analyzed. The blood counts of the son and parents of the patient were normal (data not shown).

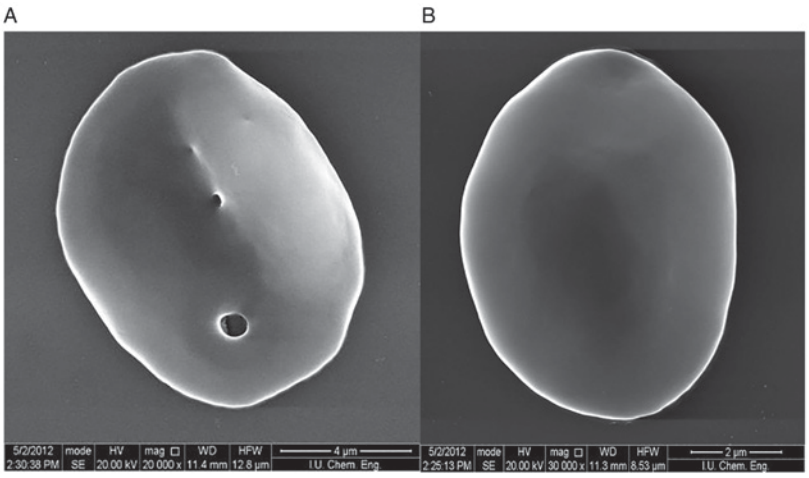

Figure 2. SEM images. Coverslipped wells were dried overnight at room temperature for SEM analysis. The samples were then covered with 5 nm gold-palladium and scanning was performed in low voltage and low vacuum mode. (A) Erythrocyte of the patient with hereditary spherocytosis (magnification, x20,000). (B) Healthy erythrocyte (magnification, x30,000). SEM, scanning electron microscopy.

Exome capture/exome sequencing analysis pipeline. Raw sequencing data were aligned to the human genome hg19 reference using Burrows-Wheeler Aligner with standard parameters in paired-end mode. SAMtools was used to remove the PCR duplicates. SAM format is a generic format for storing large nucleotide sequence alignment. SAM format is a generic alignment format or storing read aligments against reference sequences, supporting short and long reads produced by different sequencing platforms. BeDtools is an open source software package comprised of multiple tools for comparing and exploring genomic datasets via fundamental genome arithmetic tasks. BEDtools was used to calculate the coverage of targeted exome regions. A total of 82% of targeted regions were covered at least eight times, (>8% coverage) and the average sequencing depth of the regions was 24-fold (Table III). Coverage is associated with to read depth. At any given position the coverage is equal to the read depth. These values are the mean of all samples. Filtering as based on coverage. Sequencing intensity of the targeted regions increased 20 fold as determined by using Bedtools (Table III). ANNOVAR is an efficient software tool to utilize update-to-date information to functionally annotate genetic variants detected from diverse genomes. An important and probably highly desirable feature is that ANNOVAR can help identify subset of variants annotated in dbSNP or variants based on comparisons with other variant databases. ANNOVAR was used for functional information variants such as gene/exonic regions, segmental copies, SIFT and PolyPhen scores. All variants were filtered according to the following criteria are presented in Table IV. Variants were filtered based on genotype quality (GQ) score >15, read depth (DP) of >4, predicted loss-of- function or missense mutation and minor allele frequency (MAF) <0.01. Exome variant server is to discover novel genes and mechanisms contributing blood disorders by pioneering the application of NGS of the protein coding regions of the human genome across diverse, richly-phenotyped populations (Table IV). The results revealed that a new mutation which is not in dbSNP135 or 1000 genome MAF <0.01, and homozygous in the affected patient (S2) and heterozygous in the carrier parents (S4&S5); GQ >15 and coverage (DP) >4 (chr9:80000000-118000000).

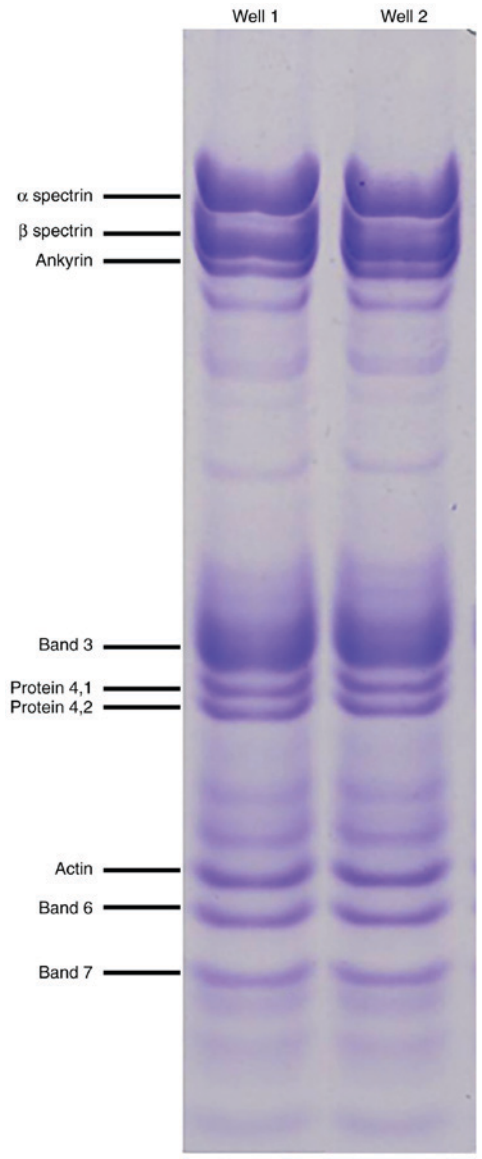

Figure 3. SDS-PAGE analysis of erythrocyte membrane proteins. Erythrocyte membrane proteins were scanned using SDS-PAGE. Well 1, healthy erythrocyte membrane proteins of the control group. Well 2, erythrocyte membrane proteins of the patient.

Table II. Quantification of erythrocyte membrane proteins of the patient and healthy controls using MALDI TOF MS.

Erythrocyte membrane proteins	Patient, ng	Healthy control, ng
CAH1; HUMAN; Carbonic anhydrase 1; OS *Homo sapiens*; GN CA1; PE 1; SV 2	0.1272	-
IGKC; HUMAN; Ig kappa chain C region; OS *Homo sapiens*; GN IGKC; PE 1; SV 1	0.1026	0.5685
P01857	0.2131	1.2857
IGHG1; HUMAN; Ig gamma 1 chain C region; OS *Homo sapiens*; GN IGHG1; PE 1; SV 1	0.2131	1.2857
P01859	-	1.0083
IGHG2; HUMAN; Ig gamma 2 chain C region; OS *Homo sapiens*; GN IGHG2; PE 1; SV 2	-	1.0083
P02549	-	44.1543
SPTA1; HUMAN; Spectrin alpha chain erythrocytic 1; OS *Homo sapiens*; GN SPTA1; PE 1; SV 5	-	44.1543
SPTA1; HUMAN; Isoform 2 of Spectrin alpha chain erythrocytic 1; OS *Homo sapiens*; GN SPTA1	13.1225	11.9537
GLPA; HUMAN; Glycophorin A; OS *Homo sapiens*; GN GYPA; PE 1; SV 2	0.9468	1.6933
P02730	30.0719[a]	137.5161
B3AT; HUMAN Band 3 anion transport protein; OS *Homo sapiens*; GN SLC4A1; PE 1; SV 3	30.0719	137.5161
P04406	3.9705	15.03
G3P; HUMAN; Glyceraldehyde 3 phosphate dehydrogenase; OS *Homo sapiens*; GN GAPDH; PE 1; SV 3	3.9705[a]	15.03
P06753-2	0.1604	0.6265
TPM3; HUMAN; Isoform 2 of Tropomyosin alpha 3 chain; OS *Homo sapiens*; GN TPM3	0.1604	0.6265
GTR1; HUMAN; Solute carrier family 2 facilitated glucose transporter member 1; OS *Homo sapiens*; GN SLC2	1.7362	5.4405
P11277	14.1724[a]	49.0578
SPTB1; HUMAN; Spectrin beta chain erythrocytic; OS *Homo sapiens*; GN SPTB; PE 1; SV 5	14.1724	49.0578
SPTB1; HUMAN; Isoform 2 of Spectrin beta chain erythrocytic; OS *Homo sapiens*; GN SPTB	-	7.4763
SPTB1; HUMAN; Isoform 3 of Spectrin beta chain erythrocytic; OS *Homo sapiens*; GN SPTB	-	1.812
ANK1; HUMAN; Ankyrin 1; OS *Homo sapiens*; GN ANK1; PE 1; SV 3	-	9.8798
P16157-12	-	46.714
ANK1; HUMAN; Isoform Er11 of Ankyrin 1; OS *Homo sapiens*; GN ANK1	-	46.714
ANK1 HUMAN; Isoform Er3 of Ankyrin 1; OS *Homo sapiens*; GN ANK1	8.6526	
EPB42; HUMAN; Isoform Long of Erythrocyte membrane protein band 4 2; OS *Homo sapiens*; GN EPB42	1.5063[a]	6.1724
STOM; HUMAN; Erythrocyte band 7 integral membrane protein; OS *Homo sapiens*; GN STOM; PE 1; SV 3	1.0081[a]	4.2655
TMOD1; HUMAN; Tropomodulin 1; OS *Homo sapiens*; GN TMOD1; PE 1; SV 1	0.2535	1.3899
P35612	-	2.7708
ADDB; HUMAN; Beta adducing; OS *Homo sapiens*; GN ADD2; PE 1; SV 3	-	2.7708
ACTG; HUMAN; Actin cytoplasmic 2; OS *Homo sapiens*; GN ACTG1; PE 1; SV 1	2.1885	0.0118
HBB; HUMAN; Hemoglobin subunit beta; OS *Homo sapiens*; GN HBB; PE 1; SV 2	5.3178	8.6761
HBA; HUMAN; Hemoglobin subunit alpha; OS *Homo sapiens*; GN HBA1; PE 1; SV 2	13.7438	5.569
DEMA; HUMAN; Dematin; OS *Homo sapiens*; GN EPB49; PE 1; SV 3	-	0.0599

[a]P<0.005 vs. healthy control; MALDI TOF MS, matrix-assisted laser desorption/ionization time-of-flight mass spectrometry.

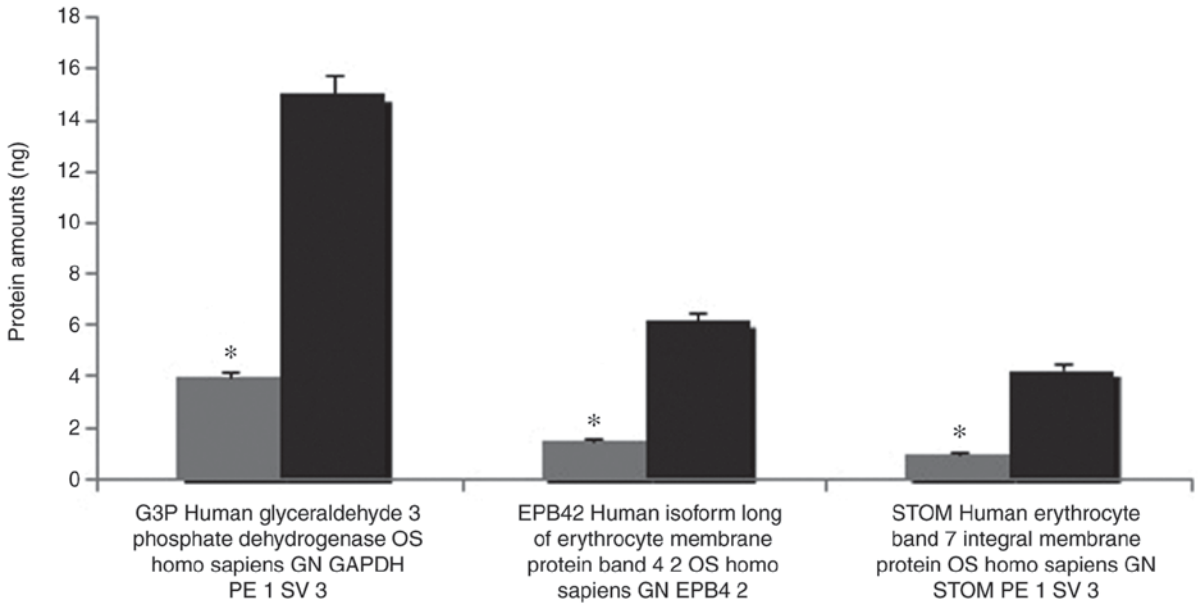

Figure 4. Erythrocyte membrane protein quantification (human glyceraldehyde-3-phosphate dehydrogenase, protein band 4.2 and band 7). The amount of erythrocyte membrane protein evaluated in the SDS-PAGE experiments was quantified using MALDI TOF MS. Grey bars denote the amount of proteins (in ng) of the patient; black bars refer to the amount of protein quantified in the erythrocytes of the control group. *P<0.05 vs. respective healthy control group. MALDI TOF MS, matrix-assisted laser desorption/ionization time-of-flight mass spectrometry.

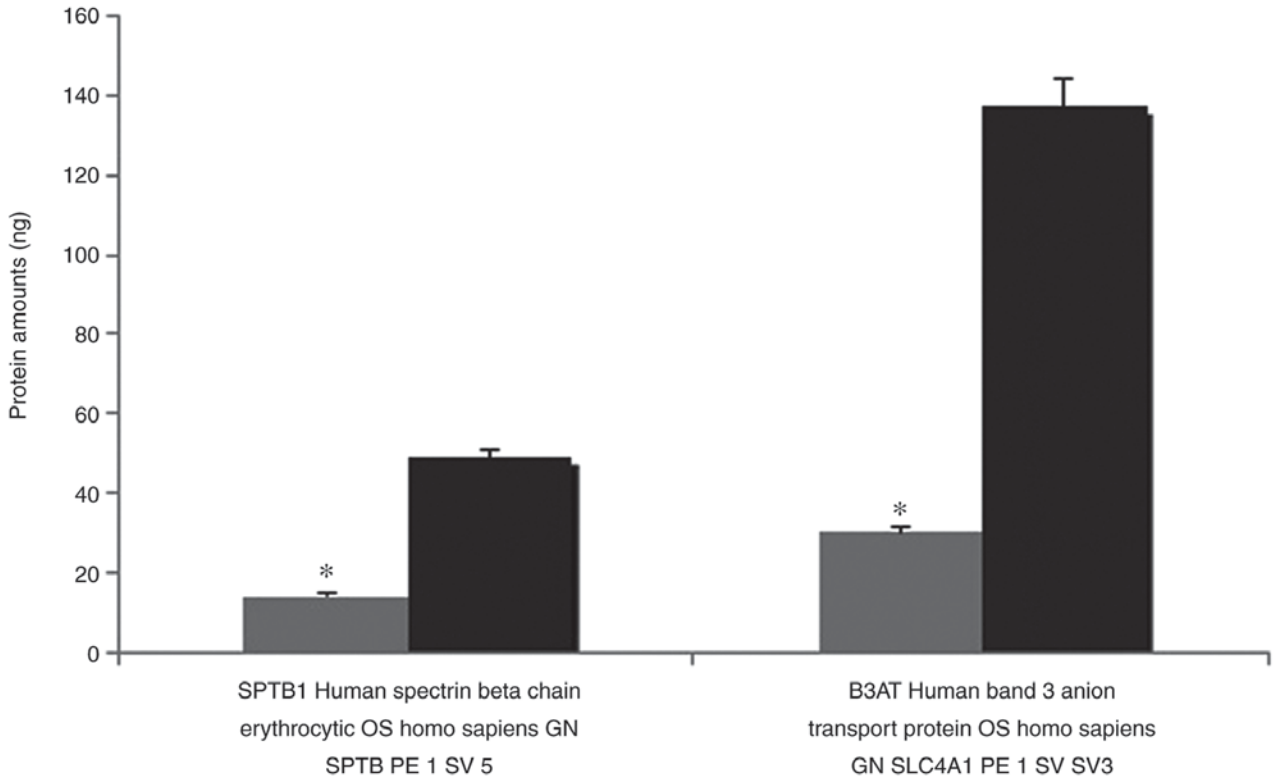

Figure 5. Erythrocyte membrane protein quantification (β-spectrin and band 3). The amount of erythrocyte membrane protein evaluated in the SDS-PAGE experiments was quantified using MALDI TOF MS. Grey bars denote the amount of proteins (in ng) of the patient; black bars refer to the amount of protein quantified in the erythrocytes of the control group. *P<0.05 vs. respective healthy control group. MALDI TOF MS, matrix-assisted laser desorption/ionization time-of-flight mass spectrometry.

From performing NGS of the genes in the present study, we examined the genetic background of the patient and her family (Table IV). Deficient proteins in the erythrocytes were identified as a result of proteomic analyses. Non-synonymous exonic mutation region was selected on GOLM1 gene (Chr9 rs142242230) after the filter was applied. SIFT, PolyPhen2, LRT and MutationTaster revealed the mutation (Table IV). Filtering of the variants according to the exon sequencing

Table III. Exome sequencing coverage analysis.

Coverage	Sample 1	Sample 2	Sample 3	Sample 4	Sample 5	Mean
Average coverage	23	25	23	22	27	24.25
>8% coverage	81%	82%	81%	80%	84%	82%

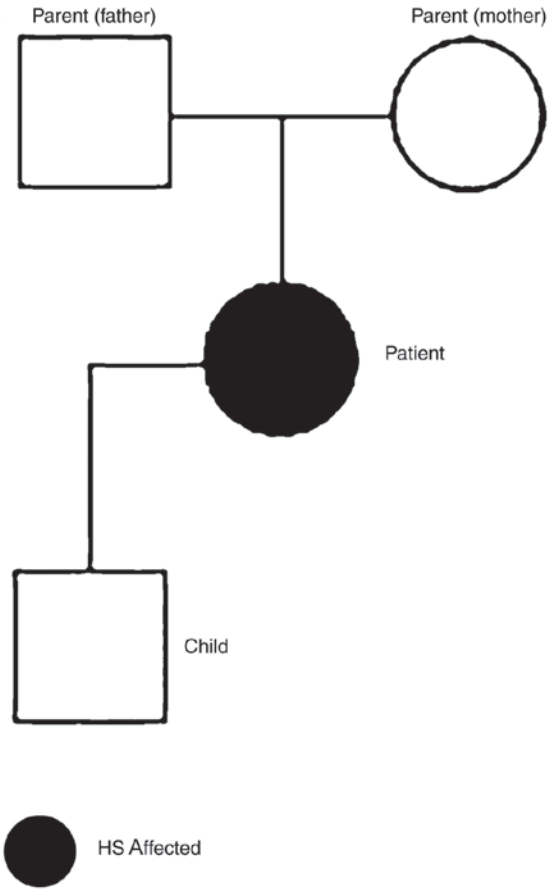

Figure 6. Family tree of the patient with HS.

of the family members and data on the family tree revealed a c.*369delA (rs34353769) point mutation 3'UTR of SPTB gene (Transcript ID: NM_001024858.2; genomic coordinates, hg19: chr14:65215655). This variation is not present in the exon sequencing of 300 Turkish individuals or in the open public database. No mutation was detected in EPB41 (band 4.1) and EPB42 (protein 4.2) genes. The workflow of exome sequencing analysis pipeline is presented in Fig. 7.

In the present study, a patient with HS aged 35 and her family were genetically analyzed and new generation sequencing was also performed, as the genetic source of HS was determined by mutation of GOLM1 gene. To determine genes and proteins that are responsible from the holes erythrocytes exome sequencing and MALDI TOF analyses were used, and the potential responsible genes and proteins were detected.

Discussion

HS is a disease accompanied by anemia, jaundice and splenomegaly due to an increased predisposition to hemolysis. It is also accompanied by a transformation of erythrocytes from biconcave and disc-shaped cells into sphere-shaped (spherocyte) cells (1). The biconcave disc-shape of erythrocytes helps to increase gas exchange with maximum efficiency at the membrane level (2). In addition, a flexible cytoskeleton and membrane structures are required for RBCs to change shape and circulate along capillaries (4,5). Therefore, quantitative and qualitative deficiencies in erythrocyte membrane proteins, which result in lipid loss from the erythrocyte surface and decreases in the erythrocyte surface/volume ratio, affect the normal activity of these cells. Beyond deforming the normal shape of RBCs, modifications in membrane proteins may lead to degeneration in heat, mechanical instability and osmotic fragility, and decrease erythrocyte life span, all of which cause hemolytic anemia (2,3). The severity of disease ranges from mild to severe depending on the extent of the membrane defects (8,9). Previous studies have demonstrated the loss of surface area results from increased membrane fragility due to primary and secondary abnormalities in erythrocyte

Table IV. Variant filtering results for HS patient (S2) and parents (S4&S6).

Filtering condition	Variants	Synonomous	Non-synonomous	Stop gain/loss	Splicing	Frameshift indels	Non-frameshift indels	Total in EVS
Total	182,671	11,408	10,775	109	164	115	196	22,767
Not in dbSNP 135 or 1000 Genome MAF <0.01	11,927	399	857	20	42	24	21	1,363
Homozygous in patient (S2) and heterozygous in parents (S4&S5)	1,014	21	28	0	2	3	5	59
GQ>15 and DP>4	377	14	14	0	2	2	3	35
In homozygous region (chr9:80000000-118000000)	23	2	1	0	0	0	0	3

dbSNP, single nucleotide polymorphism database; MAF, minor allele frequency; GQ, genotype quality; DP, depth of data; EVS, exome variant server.

membrane proteins, particularly ankyrin, α- and β-spectrin, band 3 and protein 4.2 (4).

Deteriorations of one of the erythrocyte membranes may affect other associated proteins (7). Mutations in the cytoplasmic domain of band 3 may cause functional defects by preventing the attachment of membrane proteins to cytoskeletal proteins. Translocation of amino acids (G130A) in the cytoplasmic domain of band 3 may also affect its attachment to protein 4.2. Moreover, protein 4.2 decreases have been detected in patients with band 3 damage (8,9). Therefore, it is possible that band 3 may facilitate the attachment of protein 4.2 to the membrane. Thus, slight decreases in protein 4.2 may indicate damage in the attachment region with band 3, rather than deterioration of the protein (9).

Studies have demonstrated that RBC band 3 deterioration occurs in 30% of European patients with HS, with protein decreases in the range of 15-40% (3). HS that develops as a consequence of band 3 damage is hereditary and is generally mild compared with HS caused by ankyrin and spectrin deterioration. The majority of patients (around 80%) with band 3 loss have small amounts (1-2%) of mushroom-shaped blood cells, also termed pincers (6), an RBC morphology unique to HS patients with band 3 damage.

MALDI TOF MS analysis revealed the majority of the bands, particularly spectrin and ankyrin, were reduced in the abundance of membrane proteins compared with the controls. Band 3, which has a notable role in membrane structure, decreased 4.573-fold, and protein 4.2 decreased 4.106-fold in expression compared with healthy controls Spectrin deterioration is the most common protein alteration in patients with HS (2,3). Different degrees of spectrin loss are detected in RBCs with ankyrin and spectrin deterioration (4-6). As a result, RBCs attain the spheroid form, which results in the increase in hemolysis intensity, and decreases the durability of RBC membranes against strain stress (6). However, the general structure of the cell cytoskeleton is preserved, although the number of attachment points to actin, spectrin and protein 4.1 decreases (2,6).

In the present study, high resolution microscopic images were obtained using SEM in order to characterize the morphology of the erythrocytes of an HS patient with deep vein thrombosis, and cardiac problems. Pores were observed on erythrocyte membrane surfaces in these images.

Quantitative protein assessments were performed using MALDI TOF MS to determine membrane protein deficiencies (10). A difference was detected in the analysis of the erythrocyte membrane proteins following SDS-PAGE compared with controls. It was observed that band 3 and protein 4.2, which serve a particular role in membrane structure, were decreased 4.573 and 4.106-fold, respectively.

It was hypothesized that the pores observed in the erythrocytes of the patient developed due to a decrease in these proteins, which reside in the membrane. Thus, the second phase of the study was initiated with blood drawn from the patient and the family, namely the father, mother and 12-year-old son. Proteomic analysis of isolated erythrocyte ghosts from all four individuals was performed to elucidate the cause of the disease.

The genetic profile of the patient and her family was generated via NGS, and it was concluded that a GOLM1 gene

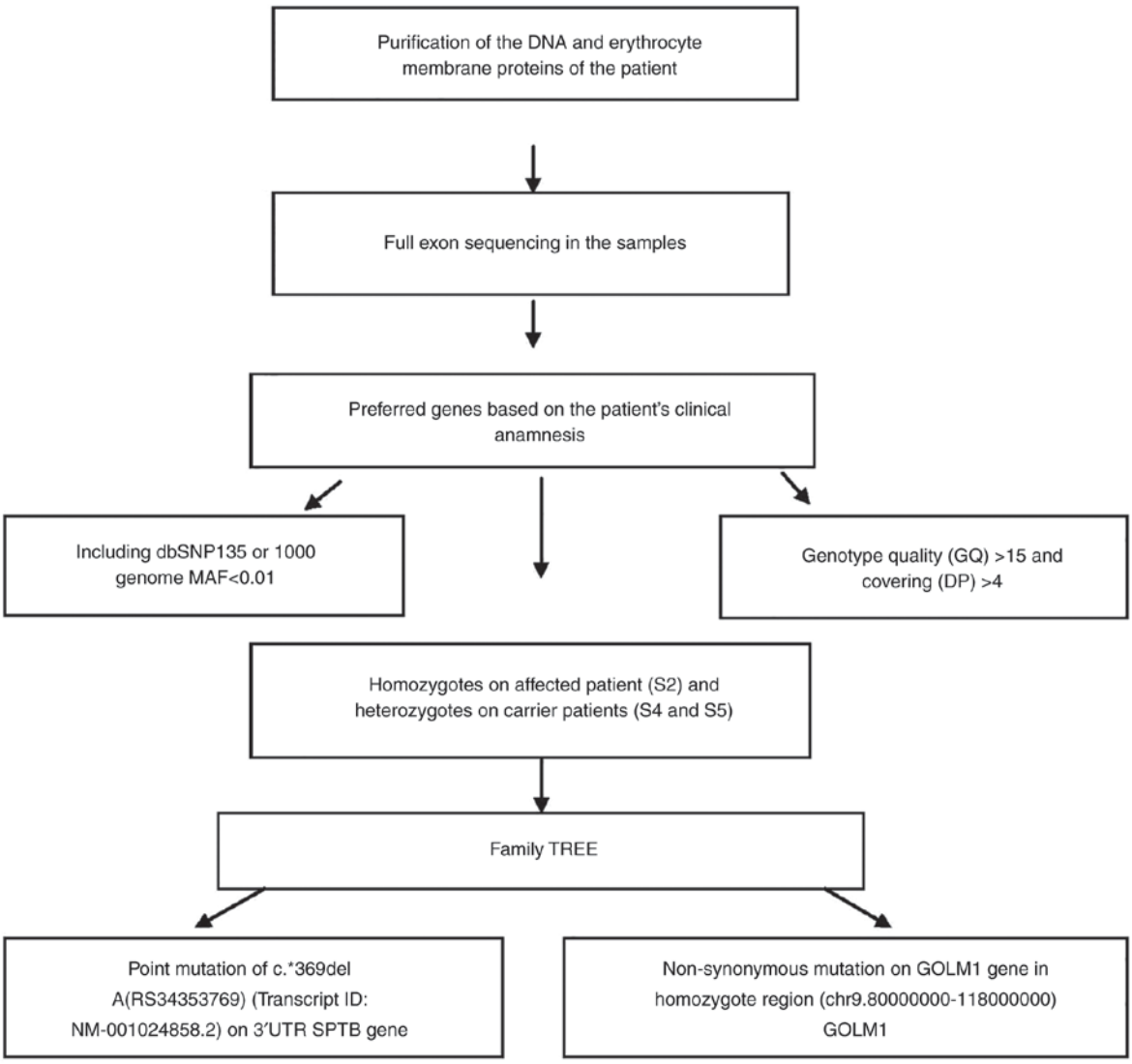

Figure 7. Analysis pipeline of exome sequencing. dbSNP, single nucleotide polymorphism database; MAF, minor allele frequency; DP, depth of data; UTR, untranslated region; SPTB, β-spectrin; GOLM1, Golgi membrane protein 1.

mutation was responsible for the emergence of the disease. Even though various hereditary conditions have specific molecular defects which are unique to a family, molecular analyses ought to be performed in severe cases where prenatal diagnosis is required. Moreover, complete genetic profiling of unique HS phenotypes may help further the understanding of the illness and provide novel insights for scientific investigation.

Acknowledgements

Not applicable.

Funding

The present study was supported by the research fund of Istanbul University (grant no. 35214).

Availability of data and materials

All data generated or analyzed during this study are included in this published article.

Authors' contributions

IA and GA contributed equally in preparing and writing this manuscript. LTS, AS, DU, GA and MA performed the experiments. IA and GA analyzed the data. All authors have reviewed and approved the final version of the article.

Ethics approval and consent to participate

The Ethics Committee of the Istanbul Faculty of Medicine, Istanbul University (Istanbul, Turkey) approved the study, and written informed consent was obtained from all subjects prior to sample collection.

Patient consent for publication

Not applicable.

Competing interests

The authors declare that they have no competing interests.

References

1. Bolton-Maggs PH, Stevens RF, Dodd NJ, Lamont G and Tittensor P and King MJ; General Haematology Task Force of the British Committee for Standards in Haematology: Guidelines for the diagnosis and management of hereditary spherocytosis. Br J Haematol 126: 455-474, 2004.
2. Perrotta S, Gallagher PG and Mohandas N: Hereditary spherocytosis. Lancet 372: 1411-1426, 2008.
3. Hug S, Pietroni ACM, Rahman H and Alam TM: Hereditary spherocytosis. J Health Popul Nutr 28: 107-109, 2010.
4. Miraglia del Giudice E, Francese M, Nobili B, Morle L, Cutillo S, Delaunay J and Perrotta S: High frequency of de novo mutations in ankyrin gene (ANK1) in children with hereditary spherocytosis. J Pediatr 132: 117-120, 1998.
5. Miraglia Del Giudice E, Lombardi C, Francese M, Nobili B, Conte ML, Amendola G, Cutillo S, Iolascon A and Perrotta S: Frequent de novo monoallelic expression of beta-spectrin gene (SPTB) in children with hereditary spherocytosis and isolated spectrin deficiency. Br J Haematol 101: 251-254, 1998.
6. Gallagher PG: Abnormalities of the erythrocyte membrane. Pediatr Clin North Am 60: 1349-1362, 2013.
7. Mohandas N and Gallagher PG: Red cell membrane: Past, present and future. Blood 112: 3939-3948, 2008.
8. Barcellini W, Fermo P, Imperiali E, Imperiali FG, Marcello AP, Vercellati C, Zaninoni A and Zanella A: Hereditary red cell membrane defects: Diagnostic and clinical aspects. Blood Transfus 9: 274-227, 2011.
9. Farias MG: Advances in laboratory diagnosis of hereditary spherocytosis. Clin Chem Lab Med 55: 944-948, 2017.
10. Karas M and Hillenkamp F: Laser desorption ionization of proteins with molecular masses exceeding 10,000 daltons. Anal Chem Oct 60: 2299-2301, 1988.
11. Gormez Z, Bakir-Gungor B and Sagiroglu MS: HomSI: Homozygous stretch identifier from next-generation sequencing data. Bioinformatics 30: 445-447, 2014.
12. Godal HC, Elde AT, Nyborg N and Brosstad F: The normal range of osmotic fragility of red blood cells. Scand J Haematol 25: 107-112, 1980.
13. Dodge JT, Mitchell C and Hanahan DJ: The preparation and chemical characteristics of hemoglobin-free ghosts of human erythrocytes. Arch Biochem Biophys 100: 119-130, 1963.
14. Laemmli UK: Cleavage of structural proteins during the assembly of the head of bacteriophage T4. Nature 227: 680-685, 1970.
15. Fan XH, Feng GD, Yang YN, Dai W and Zhao G: Diagnostic value of may grunwald giemsa staining of cerebrospinal fluid in patients with crptococcal meningitis. J Int Neurol Neurosurg 40: 220-222, 2013.
16. Wisniewski JR, Zougman A, Nagaraj N and Mann M: Universal sample preparation method for proteome analysis. Nat Methods 6: 359-362, 2009.
17. Hacariz O, Sayers G and Baykal AT: A proteomic approach to investigate the distribution and abundance of surface and internal fasciola hepatica proteins during the chronic stage of natural liver fluke infection in cattle. J Proteome Res 11: 3592-3604, 2012.
18. The UniProt Consortium: UniProt: The universal protein knowledgebase. Nucleic Acids Res 46: D158-D169, 2017.
19. Jeppsson JO, Laurell CB and Franzen B: Agarose gel electrophoresis. Clin Chem 25: 629-638, 1979.
20. Li H and Durbin R: Fast and accurate short read alignment with Burrows–Wheeler transform. Bioinformatics 25: 1754-1760, 2009.
21. Li H, Handsaker B, Wysoker A, Fennell T, Ruan J, Homer N, Marth G and Abecasis G; Durbin R and 1000 Genome Project Data Processing Subgroup: The sequence alignment/map format and SAMtools. Bioinformatics (Oxford, England) 25: 2078-2079, 2009.
22. Quinlan AR and Hall IM: BEDTools: A flexible suite of utilities for comparing genomic features. Bioinformatics 26: 841-842, 2010.
23. DePristo MA, Banks E, Poplin R, Garimella KV, Maquire JR, Hartl C, Philippakis AA, del Angel G, Rivas MA, Hanna M, *et al*: A framework for variation discovery and genotyping using next-generation DNA sequencing data. Nat Genet 43: 491-498, 2011.
24. Warden CD, Adamson AVV, Neuhausen SL and Wu X: Detailed comparison of two popular variant calling packages for exome and targeted exon studies. Peer J 30: e600, 2014.
25. Wang K, Li M and Hakonarson H: ANNOVAR: Functional annotation of genetic variants from high-throughput sequencing data. Nucleic Acids Res 38: e164, 2010.
26. Schwarz JM, Rödelsperger C, Schuelke M and Seelow D: MutationTaster evaluates disease- causing potential of sequence alterations. Nat Methods 7: 575-576, 2010.